

1 **Cell type-specific differences in redox regulation and**
2 **proliferation after low UVA doses**

3

4

5 Sylvia Ciesielska¹, Patryk Bil¹, Karolina Gajda¹, Aleksandra Poterala-

6 Hejmo¹, Dorota Hudy¹, Joanna Rzeszowska-Wolny^{1*}

7

8

9

10 ¹Biosystems Group, Institute of Automatic Control, Silesian University of Technology,
11 Gliwice, Poland

12

13

14

15 * Corresponding author

16 E-mail: joanna.rzeszowska@polsl.pl (J.R-W)

17

18

20 Abstract

21 Ultraviolet A (UVA) radiation is harmful for living organisms but in low doses may
22 stimulate cell proliferation. Our aim was to examine the relationships between exposure
23 to different low UVA doses, cellular proliferation, and changes in cellular reactive
24 oxygen species levels. In human colon cancer (HCT116) and melanoma (Me45) cells
25 exposed to UVA doses comparable to environmental, the highest doses (30-50 kJ/m²)
26 reduced clonogenic potential but some lower doses (1 and 10 kJ/m²) induced
27 proliferation. This effect was cell type and dose specific. In both cell lines the levels of
28 reactive oxygen species and nitric oxide fluctuated with dynamics which were
29 influenced differently by UVA; in Me45 cells decreased proliferation accompanied the
30 changes in the dynamics of H₂O₂ while in HCT116 cells those of superoxide. Genes
31 coding for proteins engaged in redox systems were expressed differently in each cell
32 line; transcripts for thioredoxin, peroxiredoxin and glutathione peroxidase showed
33 higher expression in HCT116 cells whereas those for glutathione transferases and
34 copper chaperone were more abundant in Me45 cells. We conclude that these two cell
35 types utilize different pathways for regulating their redox status. Many mechanisms
36 engaged in maintaining cellular redox balance have been described. Here we show that
37 the different cellular responses to a stimulus such as a specific dose of UVA may be
38 consequences of the use of different redox control pathways. Assays of superoxide and
39 hydrogen peroxide level changes after exposure to UVA may clarify mechanisms of
40 cellular redox regulation and help in understanding responses to stressing factors.

41

42

43

44

45

46 **Introduction**

47 Ultraviolet radiation is the non-ionizing part of the electromagnetic radiation spectrum
48 with a wavelength of 100-400 nm, invisible to human sight. The sun is a natural emitter
49 of UV divided into three main fractions UVA (315-400 nm), UVB (280-315 nm), and
50 UVC (100-280 nm), but most of this radiation is blocked by the atmosphere (1,2). UVA
51 constitutes the largest part (~95%) of UV radiation that reaches the Earth's surface (3),
52 whereas UVB represents only 4-5% (1). In irradiated humans UVA reaches the dermis
53 and hypodermis and has no direct impact on DNA, but it can influence cellular
54 structures indirectly by induction of reactive oxygen species (ROS) which can damage
55 macromolecules (4,1). For a long time UV was regarded as damaging for cells and
56 organisms (5), but since a few decades it is known that low doses can also stimulate
57 proliferation of cells; however, the mechanisms underlying this phenomenon are not
58 completely understood (3,1,6,7).

59 Studies of signaling pathways in conditions where UVA stimulates cell proliferation
60 show changes in the levels of proteins engaged in controlling proliferation such as
61 cyclin D1 (8,9), Pin1 (3), and Kin17 (10) or activation of epidermal growth factor
62 receptor (EGFR) which is strongly mitogenic in many cell types (8). Experiments on
63 mice showed that UVA can accelerate tumor growth (2,11).

64 One effect of exposure to UV is induction of ROS in cells, including different reactive
65 molecules and free radicals derived from molecular oxygen (12) which together with
66 reactive nitrogen species (RNS) play important roles in regulation of cell signaling and
67 survival (reviewed in 13). ROS can exert opposing effects, inducing cell damage and
68 death or stimulating proliferation by protein modifications and participation in signaling

69 pathways (14-23). Many complex mechanisms guard redox homeostasis, the balance
70 between generation and elimination of ROS and antioxidant systems, such
71 as superoxide dismutase, catalase or glutathione peroxidases which participate in these
72 control systems (24,22). The role of ROS in stimulating proliferation by low doses of
73 UVA was supported by experiments in which irradiation with a low-power diode laser
74 increased ROS production accompanied by increased cell proliferation which was
75 prevented by addition of catalase or superoxide dismutase (9), suggesting that ROS are
76 at least partly involved in stimulating proliferation (19). ROS in cells originate both
77 from external sources and as byproducts of cellular processes (24, 9, 20, 21). Low
78 levels of ROS stimulate cell proliferation by activating signaling pathways connected
79 with growth factors, causing increased cell cycle progression, while higher levels show
80 toxic effects causing cell death or senescence (24, 25). RNS include nitric oxide (NO), a
81 highly reactive gas synthesized from L-arginine by members of the nitric oxide synthase
82 (NOS) family (26). NO modulates many cellular functions (27) by acting
83 as a messenger for paracrine and autocrine communication and its production and
84 degradation are strictly controlled in different cell types (28). All cells of multicellular
85 organisms produce superoxide and NO, which appear to be the main radicals
86 responsible for the regulation of cellular redox homeostasis. This regulation is
87 especially important in the presence of external ROS sources, because cells do not
88 distinguish between endogenously- and exogenously-generated ROS. The main
89 endogenous sources of superoxide are electron leakage from the mitochondrial
90 respiratory chain and NADPH oxidases (NOXs), a family of enzymes dedicated to the
91 production of ROS in a variety of cells and tissues (reviewed in 29, 20, 30). The
92 generation of superoxide is highly conserved across all eukaryotic life and is strictly
93 regulated by antioxidant enzymes and reducing agents (13,29), and the fluctuating level

94 of ROS in cells has been postulated to be an important mechanism regulating
95 progression through the cell cycle (31, 20, 22, 32).

96 As ROS and NO play an important role in many intra- and inter-cellular signaling
97 pathways, participate in regulation of the cell cycle (reviewed in 20), and show
98 increased levels after UV radiation (4) we have studied if and how changes in their
99 levels in irradiated cells could be related to the effects of UVA on proliferation, using
100 human melanoma (Me45) and colon cancer (HCT116) cells irradiated with UVA. We
101 show that some low doses, specific for each cell line, stimulate clonogenic survival
102 whereas other, even lower doses inhibit proliferation. Comparison of the changes in the
103 intracellular levels of ROS, NO, and superoxide (O_2^-) after irradiation with stimulating,
104 suppressing, or neutral UVA doses suggests that these cell lines regulate their ROS
105 levels by different pathways, and that it is the dynamics of superoxide or H_2O_2 levels
106 which plays a crucial role in growth stimulation or inhibition.

107 **Materials and methods**

108 **Cell lines and culture**

109 Human melanoma cells (Me45, established in the Center of Oncology in Gliwice from
110 a lymph node metastasis of skin melanoma; 33) and human colorectal carcinoma cells
111 (HCT116; p53+/+, ATCC) were maintained in DMEM/F12 medium (PAN Biotech,
112 Aidenbach, Germany, cat, #P04-41150) enriched with 10% fetal bovine serum (EURx,
113 Gdansk, Poland cat# E5050-03-500) at 37 °C in a humidified atmosphere enriched in
114 5% CO_2 . The cells, 1000-5000 per dish, were irradiated at room temperature (21°C) in
115 culture plates (Sarstedt, Numbrecht, Germany cat# 83.3900) (covers opened) with
116 various doses (0.05–50 kJ/m²) of UVA (365 nm) generated by a UV crosslinker (model
117 CL-1000, UVP, Upland, CA, USA) and used for clonogenic survival assays.

118 **Clonogenic survival assays**

119 Control and irradiated cells were seeded in 60-mm dishes at 1000-5000 cells/dish and
120 incubated from 5 to 14 days (depending on the cell line) at 37°C in a humidified
121 atmosphere. The colonies were fixed with 2 ml cold 96% ethanol for 3 min, than
122 washed with PBS (PAN Biotech., Aidenbach, Germany, cat. no. P04-36500) and
123 stained with 0.5% methylene blue in 50% ethanol. Cells in colonies containing more
124 than 50 cells (estimated under the microscope) were counted and the surviving fraction
125 was calculated as the plating efficiency of irradiated cells relative to that of control un-
126 irradiated cells.

127 **Intracellular reactive oxygen species levels**

128 To quantitate intracellular ROS, 100.000 cells were seeded, growing cells were
129 collected by trypsinization, suspended in culture medium to which 2',7'-
130 dichlorofluorescein diacetate (DCFH-DA; Sigma-Aldrich, St. Louis, USA, Cat#287810)
131 was added to final concentration of 30µM. Cells were incubated for 30 min at 37°C in
132 the dark, washed with medium, suspended in PBS, and kept for 15 min on ice in the
133 dark. Fluorescence was measured by flow cytometry (Becton Dickinson FACS Canto)
134 using the FITC configuration (488 nm laser line, LP mirror 503, BP filter 530/30),
135 usually 10,000 cells were assayed per sample. To assess superoxide radicals in living
136 cells, MitoSox Red fluorogenic reagent (Thermo Fisher Scientific, Waltham, USA, cat.
137 no. M36008) was used (34, 35). Cells were collected, suspended in PBS (20,000
138 cells/300µl), incubated with MitoSox Red (5 µM final concentration) for 20 min at
139 37°C in the dark, and washed and resuspended in PBS. Samples were kept on ice until
140 analysis by flow cytometry (Becton Dickinson FACS Canto, 488 nm laser line, LP
141 mirror 566, BP filter 585/42), measuring 10,000 cell per sample. To assess NO, cells

142 were incubated with 1 μ M 4-amino-5-methylamino-2',7'-difluorescein diacetate (DAF-
143 FM, Thermo Fisher Scientific, Waltham, USA, cat.# D23844) for 30 min in dark
144 conditions at 37°C and washed with PBS. The fluorescence intensity of 10,000 cells
145 was measured by flow cytometry using the FITC configuration (488 nm laser line. LP
146 mirror 503, BP filter 530/30).

147 Results are expressed as mean fluorescence intensities \pm SD from three independent
148 experiments.

149 **Fluorescence microscopy and image analysis**

150 Fluorescent microscopy assays of superoxide and NO were performed with the same
151 fluorescent reagents as for cytometry (MitoSOX Red and DAF-FM diacetate, Thermo
152 Fisher Scientific, Waltham, USA). HCT116 and Me45 cells were seeded at 10,000 cells
153 per well in 4-well cell culture chambers (Sarstedt, Numbrecht, Germany, cat#
154 94.6140.402), grown in DMEM medium supplemented with 10% fetal bovine serum for
155 24 hours at 37°C in standard conditions, and labelled with MitoSOX Red (2.5 μ M) in the
156 first well, DAF-FM Diacetate (2.5 μ M) in the second well, both dyes in the third well,
157 and no dye in the last (control) well. Cells were incubated for 20 minutes at 37°C in a
158 humidified atmosphere enriched with 5% CO₂, the culture medium was removed, the
159 cells were washed with PBS, fixed with 0.5 ml of cold 70% ethanol per well for 10
160 minutes, and washed with the same volume of deionized water for 3 minutes. Slides
161 with fixed cells were covered with mounting gel and a cover glass. Images were
162 captured with an Olympus BX43 microscope with a 40x objective and a CoolLED
163 precisExcite fluorescence excitation system. Red and green fluorescence and transparent
164 light images were obtained for 10 areas containing cells stained with both fluorescent
165 dyes on each slide and analyzed with Matlab 2016b software using the functions

166 corrcoef() and scatter() to detect correlation between the values of corresponding pixels
167 in both fluorescence images.

168 **Expression of genes coding for proteins engaged in cellular redox** 169 **processes**

170 We identified 574 genes which are directly or indirectly engaged in redox processes,
171 using GO terms such as oxide, superoxide, nitric oxide, hydrogen peroxide, ROS and
172 reactive oxygen species. The levels of transcripts of these genes in non-irradiated
173 HCT116 and Me45 cells were extracted from our earlier Affymetrix microarray
174 experiments (32, 17) whose results are available in the ArrayExpress database under
175 accession number E-MEXP-2623. All data are MIAME compliant.

176 **Assay of total and oxidized glutathione levels**

177 For assays of total glutathione we used Rahman et al.'s modification (36) of the
178 colorimetric assay originally proposed by Vandeputte et al. (37) which is based on the
179 reaction of GSH with 5,5'-dithio-bis (2-nitrobenzoic acid) (DTNB, Sigma-Aldrich, Saint
180 Louis, USA, cat# D-8130) which produces 5-thio-2-nitrobenzoic acid (TNB) and its
181 adduct with oxidized glutathione (GS-TNB). The disulfide product was reduced by
182 glutathione reductase (0.2 U) (Sigma-Aldrich, Saint Louis, USA, cat. no. G-3664) in
183 the presence of 0.8mM NADPH (Sigma-Aldrich, Saint Louis, USA, cat. no. D-8130).
184 The TNB chromophore was measured at 412 nm in a microplate (96-plate) reader
185 (Epoch, Biotek, Winooski, USA). For measurements of oxidized glutathione (GSSG)
186 levels, cell extracts made by sonication in 0.1% Triton X-100 (Sigma-Aldrich, Saint
187 Louis, USA, cat# T8787) and 0.6% sulfosalicylic acid (Sigma-Aldrich, Saint Louis,
188 USA, cat# S-2130) in 0.05M potassium phosphate buffer pH 7.2 containing 1 mM

189 EDTA (KPE) buffer were treated with 2-vinylpyridine (Sigma-Aldrich, Saint Louis,
190 USA, cat# 132292) for 1 h at room temperature, excess 2-vinylpyridine was neutralized
191 with triethanolamine (Sigma-Aldrich, Saint Louis, USA, cat# T1377), and the
192 enzymatic recycling and reaction with DTNB was carried as described above.

193 **Statistical analyses**

194 At least three replicates of all experiments were performed and results are expressed as
195 means \pm SD and summarized as percentages relative to the appropriate controls.
196 Differences between samples were regarded as statistically significant at a p-value $<$
197 0.05 calculated by the two-sided Student t-test. Correlations between time course
198 changes in irradiated and control cells were calculated using Pearson's test and are
199 presented as correlation coefficients.

200 **Results**

201 **UVA induced proliferation changes are dose and cell-type specific**

202 HCT116 and Me45 cells were exposed to a range of UVA radiation doses (0.05, 0.1,
203 0.25, 0.5, 1, 5, 10, 15, 20, 30, 40, or 50 kJ/m²) and their proliferation was studied by
204 clonogenic tests. Some doses stimulated proliferation and others suppressed
205 proliferation when compared to un-irradiated controls in both cell lines, although they
206 responded differently and the doses that increased clonogenicity were specific for each
207 cell line (**Fig. 1**). HCT116 cells showed a statistically significant increase of colony
208 formation after exposure to 10 kJ/m² (p-value 0.02) and a decrease after 0.1, 40, and 50
209 kJ/m² (p-values 0.02, 0.05 and $<$ 0.01). The clonogenicity of Me45 cells increased after
210 irradiation with 1 and 10 kJ/m² (p-value $<$ 0.01) but was reduced after 15 to 50 kJ/m² (p-
211 values 0.01, 0.01, 0.045, 0.04 and $<$ 0.01 respectively).

212

213 **Fig 1. Clonogenicity of human cells after exposure to different UVA doses.** (A)
214 HCT116 cells, (B) Me45 cells. Data show the mean and SD of 3 experiments. Asterisks
215 denote statistical significance of differences between irradiated and control samples
216 with a p-value <0.05. The horizontal dashed line represents the control level.

217

218 **Low UVA doses do not significantly influence average levels of ROS**

219 We used specific fluorescent probes and flow cytometry to compare the levels of ROS
220 and NO in cells irradiated with different UVA doses with those in control cells. **Fig 2**
221 shows the effect of UVA on the level of superoxide detected by MitoSox, of NO
222 detected by DAF-FM, and of ROS detected by DCFH-DA. The average values for each
223 dose were calculated from all twelve assays performed in different experiments and at
224 different time points.

225

226

227 **Fig 2. Average levels of ROS and NO in HCT116 and Me45 do not significantly**
228 **change after exposure of cells to different UVA doses.** The levels were measured four
229 times during 24 h in control and cells irradiated with different UVA doses and
230 experiment was repeated 4 times. The results are presented as fold change in irradiated
231 cells versus non-irradiated controls. Data show the mean and SD of 4 experiments.

232

233 Average superoxide levels showed a tendency to increase with higher UVA dose in both
234 cell lines, but the increases were not statistically significant. NO levels did not change
235 or decreased slightly with higher doses. The levels of ROS detected with DCFH-DA
236 also did not change in irradiated HCT116 cells, but Me45 cells showed small irregular
237 increases with lower doses and decreases with higher doses. This probe detects several
238 different radicals and was first used for detection of H₂O₂ (38, 39), and it seems
239 probable that the ROS changes detected by this probe mainly reflect changes of H₂O₂

240 levels. None of the differences in average levels of ROS or NO radicals between control
241 and irradiated cells were statistically significant.

242 **ROS level dynamics change differently after different UVA doses**

243 Although the UVA doses which we used did not change the average ROS levels
244 significantly, they influenced fluctuations of these levels. The time course changes of
245 the levels of ROS assayed by DCFH-DA, of superoxide, and of NO in cells irradiated
246 with a particular dose or not irradiated are shown in **Fig 3**. Me45 and HCT116 cells
247 responded to different doses with very different kinetics of radical levels and these
248 dynamics of changes were cell type-specific. At first sight it is difficult to identify
249 features which could be correlated with the increased or decreased clonogenic potential
250 observed after irradiation with some doses.

251

252

253 **Fig 3. The dynamics of the levels of superoxide, nitric oxide and ROS detected by**
254 **DCFH-DA in control and UVA irradiated cells.** Each curve represents the results
255 after exposure to a particular UV dose shown on the right; data are means from three
256 experiments and error bars are not shown for clarity.

257

258

259 To evaluate the similarity between radical dynamics in UVA-irradiated and control
260 cells, we calculated correlation coefficients using Pearson's test. The dynamics of NO
261 levels did not change significantly after exposure of cells to any of the UVA doses
262 studied, and the increases and decreases appeared at similar time points in control and
263 irradiated cells. The correlation coefficients between cells irradiated with different doses
264 or not irradiated were >0.9 for HCT116 cells and >0.8 for three out of four doses in
265 Me45 cells (**Table 1**). This positive correlation suggests that the changes of NO levels

266 are strictly controlled in both cell lines after both stimulating or inhibiting proliferation
267 UVA doses.
268

Table 1. Correlation coefficients for the degree of similarity between radical dynamics in UV-irradiated vs. control cells			
	Superoxide¹	ROS²	NO³
<u>HCT116 cells</u>			
0.5 kJ/m ²	-0.38	0.7	1*
10 kJ/m ²	0.37	0.81	0.97*
30 kJ/m ²	-0.79	0.88	0.94*
<u>Me45 cells</u>			
0.5 kJ/m ²	0.95*	-0.01	0.89*
1 kJ/m ²	0.99*	0.59	0.89*
10 kJ/m ²	0.99*	0.83	0.93*
30 kJ/m ²	0.98*	-0.47	0.67
¹ measured by MitoSox. ² detected by DCFH-DA (mainly H ₂ O ₂). ³ measured by DAF-FM; *Pearson's correlation p-value <0.05. Bold values indicate changes from a positive to a negative correlation coefficient.			

269
270 The superoxide level dynamics in Me45 cells irradiated with any dose were highly
271 correlated with those in control cells (**Table 1**). In contrast, in HCT116 cells this level
272 showed clear differences between the effects of UVA doses which stimulated or did not
273 stimulate clonogenic potential; the dynamics of superoxide levels after doses inhibiting
274 proliferation were inversely correlated with those in control cells, while after doses
275 which stimulated proliferation these levels were positively correlated with those in
276 control cells; however the correlation coefficients were rather low. The dynamics of the
277 level of ROS in Me45 cells assayed by DCFH-DA changed after irradiation in a manner
278 similar to those of superoxide in HCT116 cells, proliferation-inhibiting doses showing a

279 negative correlation and proliferation-stimulating doses a positive correlation with the
280 dynamics in control cells.

281

282 **HCT116 and Me45 cells differ in intracellular level and localization of**
283 **NO and superoxide**

284 Me45 cells had a ~5 times lower level of NO than HCT116 cells but higher levels of
285 ROS detected by DCFH and of superoxide, as assayed by flow cytometry (**Fig 4A**).
286 Analysis of single cells using fluorescence microscopy showed that in both cell types,
287 most NO and superoxide were co-localized as shown by a high positive correlation of
288 their signals in single pixels. Rare HCT116 cells contained larger regions with a high
289 NO and a low superoxide signal (for example, Fig. 4B) but similar regions were not
290 seen in Me45 cells. Co-localization was significantly higher in Me45 than in HCT116
291 cells; Pearson's correlation coefficients for all pixels in 10 fields containing 5 to 10 cells
292 were 0.9 and 0.6 in Me45 and HCT116 cells, respectively.

293 **Fig 4. Nitric oxide and ROS in HCT116 and Me45 cells.** A; mean levels of NO,
294 superoxide and ROS detected by DCFH-DA measured in whole population of
295 unirradiated cells by flow cytometry (average from 3 experiments), B; examples of
296 superoxide and NO distribution in single HCT116 and Me45 cells observed by
297 fluorescence microscopy, NO detected by fluorescence of DAF-FM diacetate and
298 superoxide by MitoSOX Red.

299

300 **HCT116 and Me45 cells have different levels of some transcripts**
301 **participating in redox systems**

302 The differences in response to UVA and in radical levels in the two cell lines
303 suggested that they use different mechanisms for the regulation of their redox status. To
304 get more information on these mechanisms, we compared the expression of different
305 genes coding for proteins engaged directly or indirectly in redox processes in each cell

306 line. The expression levels of more than 500 candidate genes found on the basis of
307 ontology terms were compared using our earlier microarray data for Me45 and HCT116
308 cells (17). The full list of these genes and their expression levels are given in Table S1
309 of the Supplement. Both cell lines express many genes engaged in redox regulation and
310 expression of some of these genes is significantly higher in Me45 or HCT116 cells
311 (Tables 2 and 3).

312 Me45 cells contain lower levels of transcripts for thioredoxin (TXN) and peroxyredoxin
313 (PRDX) and higher levels of transcripts for thioredoxin-inhibiting protein (TXNIP). On
314 the other hand, genes coding for glutathione S-transferases (GST) show higher
315 expression in Me45 cells, with the *GSTM3* transcript showing the largest difference.
316 Transcripts for the antioxidant ATOX1, a copper chaperone which may increase activity
317 of the protein SOD1 by providing copper ions and influence *SOD3* gene expression as a
318 transcription factor (40, 41), are more than 10 times more abundant in Me45 than in
319 HCT116 cells. There are also some genes which are significantly more highly expressed
320 in HCT116 cells, for example GTP cyclohydrolase 1 which codes for the first and rate-
321 limiting enzyme in biosynthesis of tetrahydrobiopterin (BH4), a cofactor required for
322 activity of nitric oxide synthases (42,43).

323

Table 2. Genes with higher expression in Me45 than in HCT116 cells			
Gene	Gene symbol	Transcript level [a.u.]¹	Enrichment²
Glutathione S-Transferase Mu 3	<i>GSTM3</i>	299	27.0
Antioxidant 1 Copper Chaperone	<i>ATOX1</i>	3336	11.3
Thioredoxin Interacting Protein	<i>TXNIP</i>	346	10.7
Glutathione S-Transferase Alpha 4	<i>GSTA4</i>	316	3.0
Peroxidasin	<i>PXDN</i>	80	2.8

Glutathione S-Transferase Kappa 1	<i>GSTK1</i>	734	2.4
SH3 Domain Binding Glutamate Rich Protein Like 3	<i>SH3BGRL3</i>	552	2.3
Cyclin Dependent Kinase 5	<i>CDK5</i>	565	2.2
Cyclin Dependent Kinase 2	<i>CDK2</i>	359	2
Glutathione S-Transferase Pi 1	<i>GSTP1</i>	1042	1.8
Catalase	<i>CAT</i>	402	1.6
Glutathione S-Transferase Omega 1	<i>GSTO1</i>	2037	1.4
Microsomal Glutathione S-Transferase 3	<i>MGST3</i>	1334	1.2
Thioredoxin Reductase 1	<i>TXNRD1</i>	758.2	1.1
¹ arbitrary units reflect normalized data from microarray experiment. ² Fold change			

324

Table 3. Genes with higher expression in HCT116 than in Me45 cells			
Gene	Gene symbol	Transcript level¹	Enrichment²
GTP Cyclohydrolase 1 (BH4 synthesis)	<i>GCHI</i>	260	19
Dimethylarginine Dimethylaminohydrolase 1 (demethylation of arginine)	<i>DDAHI</i>	279	11
F2R Like Trypsin Receptor 1	<i>F2RL1</i>	206	9
Thioredoxin Like 1	<i>TXNL1</i>	1281	4
Glutamate-cysteine ligase regulatory subunit (glutathione synthesis)	<i>GCLM</i>	170	3.4
NAD(P)H Quinone Dehydrogenase 2	<i>NQO2</i>	515	3
Thioredoxin Related Transmembrane Protein 1	<i>TMX1</i>	397	2.5
Peroxiredoxin 2	<i>PRDX2</i>	1448	2.5
Thioredoxin	<i>TXN</i>	2269	2.4

Glutaredoxin 5	<i>GLRX5</i>	976	2.4
Nitric oxide synthase interacting protein	<i>NOSIP</i>	299	2.4
Glutaredoxin 2	<i>GLRX2</i>	329	2.2
Peroxiredoxin 3	<i>PRDX3</i>	791	1.9
Peroxiredoxin 6	<i>PRDX6</i>	1009	1.8
LanC Like 1	<i>LANCL1</i>	241	1.7
Superoxide Dismutase 1	<i>SOD1</i>	2902	1.7
Peroxiredoxin 1	<i>PRDX1</i>	2571	1.5
Nitric Oxide Synthase 2	<i>NOS2</i>	74	1.5
Peroxiredoxin 4	<i>PRDX4</i>	1303	1.4
Glutathione Peroxidase 4	<i>GPX4</i>	1331	1.2
Apurinic/Apyrimidinic Endodeoxyribonuclease 1	<i>APEX1</i>	1545	2.7
¹ arbitrary units reflect normalized data from microarray experiment. ² Fold change			

325

326 **Glutathione in HCT116 and Me45 cells**

327 Glutathione is an important player in cell redox regulation (36) and the gene *GCLM*
328 which codes for glutamate-cysteine ligase regulatory subunit, required for synthesis of
329 glutathione, is more highly expressed in HCT116 than in Me45 cells (Table 3). We
330 therefore compared the levels of reduced (GSH) and oxidized (GSSG) glutathione in
331 these cells. The levels of total glutathione, GSH (~96% of the total), and of GSSG were
332 lower in Me45 cells, but the differences were not statistically significant (**Fig 5**).

333

334

335 **Fig 5. Levels of reduced (GSH) and oxidized (GSSG) glutathione in HCT116 and**
336 **Me45 cells.** Data show the mean and SD of 3 independent experiments.

337

338 **Discussion**

339 **Stimulation of proliferation by UVA and fluctuations of intracellular** 340 **ROS level**

341 Stimulation of cell proliferation by UVA radiation at doses of 3-9 kJ/m² has been
342 known for a few decades. (9, 3). Here we show that doses in this range, but not
343 exceeding 10 kJ/m², increase the clonogenic potential of HCT116 and Me45 cells and
344 that this effect is dose- and cell type-specific (Fig. 1). We further relate this specificity
345 to cellular redox regulation, supporting a role for redox conditions and superoxide and
346 NO in regulation of proliferation which was suggested 30 years ago (44, 14, 45
347 reviewed in 46,47). We hypothesized that the induction of cell proliferation by UVA
348 may be caused by changes in intracellular levels of ROS and RNS (34, 35).

349 The levels of intracellular ROS, superoxide, and NO, assayed using specific probes,
350 changed in time (Fig 3) in agreement with the fluctuations of ROS level observed by
351 others and proposed to be important in regulation of the cell cycle (reviewed in 20). In
352 some cases the kinetics of the changes of level after irradiation were highly correlated
353 with those in control cells (Table 1); for example, in both cell types the general pattern
354 of NO level change did not vary after irradiation although their levels differed (Fig 3),
355 suggesting that the pattern of NO level change is important for regulatory mechanisms
356 in both cell types. For other radicals, the correlation between irradiated and control cells
357 was much lower and sometimes changed sign; for example, in Me45 cells the
358 fluctuations of superoxide level did not vary after irradiation and were highly correlated
359 with those in control cells, whereas in contrast the fluctuations in HCT116 cells varied

360 depending on the UVA dose and were inversely correlated with those in control cells
361 after proliferation-inhibiting doses, but were positively correlated after proliferation-
362 stimulating doses. In HCT116 cells the DCFH-DA-detected ROS level changed more
363 regularly than that in Me45 cells, while in Me45 cells irradiated with proliferation-
364 inhibiting UVA doses it became inversely correlated compared to the dynamics in
365 control cells. An increase of proliferation rate after irradiation was observed only if the
366 fluctuations of ROS level retained their pattern in control cells, although conservation of
367 the pattern of fluctuations of different radicals in both cell lines were important (Table
368 1). Overall, these results suggest that it is the pattern of fluctuations of radical levels,
369 rather than the levels themselves, which influences proliferation rate after UVA
370 irradiation and that each cell type may use different pathways to regulate cellular redox
371 status.

372 **ROS-regulating pathways and their choice in HCT116 and Me45 cells**

373 ROS participate in many signaling pathways, including those regulating the cell cycle
374 and proliferation (24, 9, 20, 22), and their intracellular levels must be precisely
375 controlled. The main players in regulation of cellular redox status are superoxide and
376 NO which are produced by cells and interact with each other and with many other
377 cellular molecules. Their levels are regulated by a series of feedback circuits, mainly
378 based on peroxiredoxins, thioredoxins, glutathione, thioredoxin and glutathione
379 reductases, NADPH, and enzymes engaged in production of superoxide or NO
380 (reviewed in 48,49,50) (**Fig 6**). Fig 6 shows some proteins whose differential expression
381 in Me45 and HCT116 cells may influence these pathways. Many other possible
382 interactions of superoxide and ONOO⁻ occur, with themselves, with other proteins, CO₂,
383 antioxidants, and other compounds which result in creation of new radicals and
384 interaction circuits which further influence the redox state of the cell and create

385 additional regulatory sub-circuits, described in detail in many recent and older reviews
386 (48,51,50,52). Nevertheless, the ROS regulatory circuits in Fig 6 seem to create the
387 basic pathways for redox regulation in cells which may determine the character of
388 radical level fluctuations.

389

390 **Fig 6. The main pathways for regulation of superoxide and NO levels in Me45 and**
391 **HCT116 cells.** A,C and E show production and further interactions of superoxide (A),
392 hydrogen peroxide (C) and peroxynitrite (E) and regulatory pathways engaged. B,D and
393 F compare use of presented regulatory pathways in HCT116 and Me45 cells by the size
394 of black (Me45) and white (HCT116) arrows.

395

396 The two main pathways leading to regulation of superoxide levels start by its
397 conversion to H₂O₂ or to peroxynitrite in reactions with NO (53,50). H₂O₂ may be
398 created by interaction of two superoxide molecules, either spontaneously or more
399 efficiently by superoxide dismutase (SOD) (53,24,22). Interaction of superoxide with
400 NO starts another pathway by creation of the very reactive peroxynitrite radical
401 (ONOO⁻); the sources of superoxide and NO and their spatial separation may determine
402 further regulatory pathways through H₂O₂ or ONOO⁻ in cells.

403 NOS produces either NO or superoxide in appropriate conditions (54), and we speculate
404 that this could explain the more frequent colocalization of these two types of radical in
405 Me45 than in HCT116 cells (**Fig 4**). All three isoforms of NOS contain the N-terminal
406 oxygenase and C-terminal reductase domains separated by a linker, and function as
407 homodimers which produce NO by oxidation of L-arginine to L-citrulline (55 reviewed
408 in 56,57). In the absence of the cofactor, tetrahydrobiopterin (BH₄), the domains
409 become uncoupled and NOS produces superoxide instead of NO (42,43,57 reviewed in
410 56). The levels of transcripts for the NOS isoforms are rather low and are similar in
411 HCT116 and Me45 cells, except that for NOS2 which is slightly higher in HCT116 cells
412 (Table 3 and Supplementary Material). However, the gene *GCHI* which encodes the

413 rate-limiting enzyme in synthesis of BH₄ (58) is expressed at a significantly lower level
414 in Me45 cells (Table 3) which could result in insufficient availability of BH₄ and
415 consequently an increased production of superoxide by NOS. Further, in Me45 cells the
416 level of transcripts for glutathione transferases is significantly higher (Table 2) and
417 glutathionylation of NOS results in increased production of superoxide (59, 43.). Either
418 or both of these scenarios would result in superoxide forming a larger fraction of the
419 products of NOS in Me45 cells and to the observed more frequent apparent
420 colocalization with NO. This would lead to higher production of peroxynitrite which
421 may be further converted to NO₂ by peroxiredoxins and glutathione peroxidases which
422 also participate in reduction of H₂O₂ (60, 61) and these pathways are probably used
423 preferentially by HCT116 cells which show higher expression of PRDX, TXN, GPX
424 than Me45 cells. The other pathway for ONOO⁻ reduction is interaction with transition
425 metal centers (reviewed in 48) and Me45 cells show significantly higher levels than
426 HCT116 cells of *ATOX* gene transcripts coding for copper chaperone (62,22) and of
427 transcripts of thioredoxin-inhibiting protein TXNIP, suggesting that in Me45 cells
428 interaction of ONOO⁻ with transition metals may be dominating.

429 Glutathione is a further important player in redox regulation, and its level is lower in
430 Me45 cells than in HCT116 cells (Fig 5). This could plausibly be due to the lower
431 expression of the *GCLM* gene (Table 3), or to greater use of glutathione for
432 glutathionylation of proteins since genes coding for GSTs are more highly expressed in
433 Me45 cells. As glutathione is necessary for reactivation of GPX, one could again expect
434 that the pathway engaging GPX will be also less efficient in Me45 cells.

435 Redox balance plays a critical role in regulating biological processes and many cellular
436 pathways, including stimulation and inhibition of proliferation, are influenced by ROS
437 levels. Our results suggest that cells may concentrate on strict regulation of superoxide

438 or hydrogen peroxide levels when changed by stress, and that stimulation or inhibition
439 of cell proliferation depend on the dynamics of level fluctuations and less on the ROS
440 levels themselves. We show for the first time that varying responses of different cell
441 types to the same stimulus such as a specific dose of UVA may result from their use of
442 different redox control pathways.

443

444 **Acknowledgments**

445 This work was supported by the Polish National Science Center Grant
446 2015/19/B/ST7/02984.

447 Ronald Hancock (Laval University, Québec, Canada) is acknowledged for critically
448 reading and editing the manuscript.

449

450 **References**

- 451 1. IARC Working Group Reports. Vol 1. Exposure to artificial UV radiation and
452 skin cancer. ISBN 92 832 2441 8, 2005
- 453 2. Sluyter R, Halliday GM. Enhanced tumor growth in UV-irradiated skin is
454 associated with an influx of inflammatory cells into the epidermis.
455 *Carcinogenesis* 21: 1801-1807, 2000
- 456 3. Han CY, Hien TT, Lim SC, Kang KW. Role of Pin1 in UVA-induced cell
457 proliferation and malignant transformation in epidermal cells. *Biochem Biophys*
458 *Res Commun.* 410: 68-74, 2011
- 459 4. Bachelor MA, Bowden GT. UVA-mediated activation of signaling pathways
460 involved in skin tumor promotion and progression. *Semin Cancer Biol.* 14:131-
461 8, 2004

- 462 5. Berton TR, Mitchell DL, Fischer SM, Locniskar MF. Epidermal proliferation
463 but not quantity of DNA photodamage is correlated with UV-induced mouse
464 skin carcinogenesis. *J Invest Dermatol.* 109:3407, 1997
- 465 6. Liu Z, Chen H, Yang H, Liang J, and Li X. Low-Dose UVA Radiation-Induced
466 Adaptive Response in Cultured Human Dermal Fibroblasts. *International*
467 *Journal of Photoenergy* 2012, ID 167425, 2012.
- 468 7. WHO. Global Solar UV index. ISBN 92 4 159007 6, 2002
- 469 8. El-Abaseri TB, Putta S, Hansen LA. Ultraviolet irradiation induces keratinocyte
470 proliferation and epidermal hyperplasia through the activation of the epidermal
471 growth factor receptor. *Carcinogenesis* 27:225-31, 2006
- 472 9. Grossman N, Schneid N, Reuveni H, Halevy S, Lubart R. 780 nm low power
473 diode laser irradiation stimulates proliferation of keratinocyte cultures:
474 involvement of reactive oxygen species. *Lasers Surg Med.* 22: 212-8, 1998
- 475 10. Kannouche P, Pinon-Lataillade G, Tissier A, Chevalier-Lagente O, Sarasin
476 A, Mezzina M, Angulo JF. The nuclear concentration of kin17, a mouse protein
477 that binds to curved DNA, increases during cell proliferation and after UV
478 irradiation. *Carcinogenesis.* 19: 781-9, 1998
- 479 11. Staberg B, Wulf HC, Klemp P, Poulsen T, Brodthagen H. The carcinogenic
480 effect of UVA irradiation. *Journal of Investigative Dermatology* 81: 517-519,
481 1983
- 482 12. Bossi O, Gartsbein M, Leitges M, Kuroki T, Grossman S, Tennenbaum T. UV
483 irradiation increases ROS production via PKCdelta signaling in primary murine
484 fibroblasts. *J Cell Biochem.* 105: 194-207, 2008
- 485 13. Aguirre J, Lambeth JD. Nox enzymes from fungus to fly to fish and what they
486 tell us about Nox function in mammals. *Free Radic Biol Med.* 49:1342-53, 2010.

- 487 14. Burdon RH. Superoxide and hydrogen peroxide in relation to mammalian cell
488 proliferation. *Free Radic Biol Med.* 18:775-94, 1995
- 489 15. Foksinski M, Zarakowska E, Gackowski D, Skonieczna M, Gajda K, Hudy D,
490 Szpila A, Bialkowski K, Starczak M, Labejszo A, Czyz J, Rzeszowska-Wolny J,
491 Olinski R. Profiles of a broad spectrum of epigenetic DNA modifications in
492 normal and malignant human cell lines: Proliferation rate is not the major factor
493 responsible for the 5-hydroxymethyl-2'-deoxycytidine level in cultured
494 cancerous cell lines. *PLoS One* 12: e0188856, 2017
- 495 16. Irani K. Oxidant signaling in vascular cell growth, death, and survival: a review
496 of the roles of reactive oxygen species in smooth muscle and endothelial cell
497 mitogenic and apoptotic signaling. *Circ Res.* 87: 179-83, 2000
- 498 17. Jaksik R, Lalik A, Skonieczna M, Cieslar-Pobuda A, Student S, Rzeszowska-
499 Wolny J. MicroRNAs and reactive oxygen species: are they in the same
500 regulatory circuit? *Mutat Res Genet Toxicol Environ Mutagen.* 764-765: 64-71,
501 2014
- 502 18. Janssen Y, Van Houten B, Borm P, Mossman B. Cell and tissue responses to
503 oxidative damage. *Lab Investig.* 69: 261–274, 1993
- 504 19. Klotz LO, Pellieux C, Briviba K, Pierlot C, Aubry JM, Sies H. Mitogen
505 activated protein kinase (p38-, JNK-, ERK-) activation pattern induced by
506 extracellular and intracellular singlet oxygen and UVA. *Eur J Biochem.* 260:
507 917-22, 1999
- 508 20. Menon SG, Goswami PC. A redox cycle within the cell cycle: ring in the old
509 with the new. *Oncogene* 26: 1101-9, 2007
- 510 21. Murrell GA, Francis MJ, Bromley L. Modulation of fibroblast proliferation by
511 oxygen free radicals. *Biochem J.* 265: 659-65, 1990

- 512 22. Sarsour EH, Kumar MG, Chaudhuri L, Kalen AL, Goswami PC. Redox control
513 of the cell cycle in health and disease. *Antioxid Redox Signal* 11: 2985-3011,
514 2009
- 515 23. Skonieczna M, Hejmo T, Poterala-Hejmo A, Cieslar-Pobuda A, and Buldak
516 RJ. NADPH oxidases: Insights into selected functions and mechanisms of action
517 in cancer and stem cells. *Oxidative Medicine and Cellular Longevity*, vol. 2017,
518 9420539, 2017
- 519 24. Boonstra J, Post JA. Molecular events associated with reactive oxygen species
520 and cell cycle progression in mammalian cells. *Gene* 337:1-13, 2004
- 521 25. Hatanaka E, Dermargos A, Armelin HA, Curi R, Campa A. Serum amyloid A
522 induces reactive oxygen species (ROS) production and proliferation of
523 fibroblast. *Clin Exp Immunol.* 163: 362-7, 2011.
- 524 26. Villalobo A. Nitric oxide and cell proliferation. *FEBS J.* 273: 2329-44, 2006
- 525 27. Ignarro LJ, Buga GM, Wei LH, Bauer PM, Wu G, del Soldato P. Role of the
526 arginine-nitric oxide pathway in the regulation of vascular smooth muscle cell
527 proliferation. *Proc Natl Acad Sci USA* 8: 4202-8, 2001
- 528 28. Napoli C, Paolisso G, Casamassimi A, Al-Omran M, Barbieri M, Sommese L,
529 Infante T, Ignarro LJ. Effects of nitric oxide on cell proliferation: novel insights.
530 *J Am Coll Cardiol.* 62: 89-95, 2013
- 531 29. Finkel T. Signal transduction by mitochondrial oxidants. *J Biol Chem.* 287:
532 4434-40, 2012
- 533 30. Trachootham D, Lu W, Ogasawara MA, Nilsa RD, Huang P. Redox regulation
534 of cell survival. *Antioxid Redox Signal.* 10: 1343-74, 2008

- 535 31. da Veiga Moreira J, Peres S, Steyaert JM, Bigan E, Paulevé L, Nogueira ML,
536 Schwartz L. Cell cycle progression is regulated by intertwined redox oscillators.
537 Theor Biol Med Model. 12:10, 2015
- 538 32. Thomas DD, Ridnour LA, Isenberg JS, Flores-Santana W, Switzer CH, Donzelli
539 S, Hussain P, Vecoli C, Paolucci N, Ambs S, Colton CA, Harris CC, Roberts
540 DD, Wink DA. The chemical biology of nitric oxide: implications in cellular
541 signaling. Free Radic Biol Med. 45:18-31, 2008
- 542 33. Krzywon A, Widel M, Fujarewicz K, Skonieczna M, Rzeszowska-Wolny J.
543 Modulation by neighboring cells of the responses and fate of melanoma cells
544 irradiated with UVA. J Photochem Photobiol B. 178: 505-511, 2018
- 545 34. Robinson KM, Janes MS, Beckman JS. The selective detection of mitochondrial
546 superoxide by live cell imaging Nat Protoc 3: 941–47, 2008
- 547 35. Robinson KM, Janes MS, Pehar M, Monette JS, Ross MF, Hagen TM, Murphy
548 MP, Beckman JS. Selective fluorescent imaging of superoxide in vivo using
549 ethidium-based probes. Proc Natl Acad Sci USA 103: 15038–43, 2006
- 550 36. Rahman I, Kode A, Biswas SK. Assay for quantitative determination of
551 glutathione and glutathione disulfide levels using enzymatic recycling method.
552 Nat Protoc 1: 3159-31645, 200643
- 553 37. Vandeputte C, Guizon I, Genestie-Denis I, Vannier B, Lorenzon G. A microtiter
554 plate assay for total glutathione and glutathione disulfide contents in
555 cultured/isolated cells: performance study of a new miniaturized protocol. Cell
556 Biology and Toxicology 10: 415-421, 1994
- 557 38. Ubezio P, Civoli F. Flow cytometric detection of hydrogen peroxide production
558 induced by doxorubicin in cancer cells. Free Radic Biol Med. 16: 509-16, 1994

- 559 39. Arnold RS, Shi J, Murad E, Whalen AM, Sun CQ, Polavarapu R, Parthasarathy
560 S, Petros JA, Lambeth JD. Hydrogen peroxide mediates the cell growth and
561 transformation caused by the mitogenic oxidase Nox1. *Proc Natl Acad Sci U S*
562 *A* 98:5550-5, 2001
- 563 40. Culotta VC, Yang M, O'Halloran TV. Activation of superoxide dismutases:
564 putting the metal to the pedal. *Biochim Biophys Acta* 1763: 747–758, 2006
- 565 41. Ozumi K, Sudahar V, Kim H-W, Chen G-F, Kohno T, Finney L, Vogt S,
566 McKinney RD, Ushio-Fukai M, Fukai T. Role of copper transport protein
567 antioxidant 1 in angiotensin II–induced hypertension a key regulator of
568 extracellular superoxide dismutase. *Hypertension* 60: 476-486, 2012
- 569 42. Benson MA, Batchelor H, Chuaiphichai S, Bailey J, Zhu H, Stuehr DJ,
570 Bhattacharya S, Channon KM, Crabtree MJ. A pivotal role for tryptophan 447 in
571 enzymatic coupling of human endothelial nitric oxide synthase (eNOS): effects
572 on tetrahydrobiopterin-dependent catalysis and eNOS dimerization. *J Biol*
573 *Chem.* 288: 29836-45, 2013
- 574 43. Crabtree MJ, Brixey R, Batchelor H, Hale AB, Channon KM. Integrated redox
575 sensor and effector functions for tetrahydrobiopterin- and glutathionylation-
576 dependent endothelial nitric-oxide synthase uncoupling. *J Biol Chem.* 288:561-
577 9, 2013
- 578 44. Burdon RH, Gill V, Rice-Evans C. Cell proliferation and oxidative stress. *Free*
579 *Radic Res Commun.* 7:149-59, 1989
- 580 45. Ikebuchi Y, Masumoto N, Tasaka K, Koike K, Kasahara K, Miyake A,
581 Tanizawa O. Superoxide anion increases intracellular pH, intracellular free
582 calcium, and arachidonate release in human amnion cells. *J Biol Chem.* 266:
583 13233-7, 1991

- 584 46. Burdon RH. Control of cell proliferation by reactive oxygen species. *Biochem*
585 *Soc Trans.* 24:1028-32, 1996
- 586 47. Forman HJ. Redox signaling: An evolution from free radicals to aging. *Free*
587 *Radic Biol Med.* 97:398-407, 2016
- 588 48. Bartesaghi S, Radi R. Fundamentals on the biochemistry of peroxynitrite and
589 protein tyrosine nitration. *Redox Biol.* 14:618-625, 2018
- 590 49. Hanschmann EM, Godoy JR, Berndt C, Hudemann C, Lillig CH. Thioredoxins,
591 glutaredoxins, and peroxiredoxins--molecular mechanisms and health
592 significance: from cofactors to antioxidants to redox signaling. *Antioxid Redox*
593 *Signal.* 19: 1539-605, 2013
- 594 50. Radi R. Peroxynitrite, a stealthy biological oxidant. *J Biol Chem.* 288: 26464-
595 72, 2013
- 596 51. Radi R. Nitric oxide, oxidants, and protein tyrosine nitration. *Proc Natl Acad Sci*
597 *U S A.* 101: 4003-8, 2004
- 598 52. Szabo C, Ischiropoulos H, Radi R. Peroxynitrite: biochemistry, pathophysiology
599 and development of therapeutics. *Nature Rev. Drug Discovery* 6: 662-680, 2007
- 600 53. Beckman JS, Koppenol WH. Nitric oxide, superoxide, and peroxynitrite: the
601 good, the bad, and ugly. *Am J Physiol.* 271: C1424-37, 1996
- 602 54. Radi R, Cassina A, Hodara R. Nitric oxide and peroxynitrite interactions with
603 mitochondria, *Biol Chem.* 383:401-409, 2001
- 604 55. Pou S, Pou WS, Bredt DS, Snyder SH, Rosen GM. Generation of superoxide by
605 purified brain nitric oxide synthase. *J Biol Chem.* 267: 24173-6, 1992
- 606 56. Forstermann U, Sessa, WC. Nitric oxide synthases. Regulation and function.
607 *Eur. Heart J.* 33: 829-837, 2012

- 608 57. Vásquez-Vivar J, and Kalyanaraman B. Generation of superoxide from nitric
609 oxide synthase. FEBS Lett. 481: 305–306, 2000
- 610 58. Cai S, Alp NJ, McDonald D, Smith I, Kay J, Canevari L, Heales S, Channon
611 KM. GTP cyclohydrolase I gene transfer augments intracellular
612 tetrahydrobiopterin in human endothelial cells: effects on nitric oxide synthase
613 activity, protein levels and dimerisation. Cardiovasc Res. 55: 838-49, 2002
- 614 59. Chen CA, Wang TY, Varadharaj S, Reyes LA, Hemann C, Talukder MA, Chen
615 YR, Druhan LJ, Zweier JL. S-glutathionylation uncouples eNOS and regulates
616 its cellular and vascular function. Nature 468:1115–1118, 2010
- 617 60. Knoop B, Goemaere J, Van der Eecken V, Declercq JP. Peroxiredoxin 5:
618 structure, mechanism, and function of the mammalian atypical 2-Cys
619 peroxiredoxin. Antioxid Redox Signal 15: 817-29, 2011
- 620 61. Walbrecq G, Wang B, Becker S, Hannotiau A, Fransen M, Knoop B.
621 Antioxidant cytoprotection by peroxisomal peroxiredoxin-5. Free Radic Biol
622 Med. 84: 215-226, 2015
- 623 62. Hatori Y, Inouye S, Akagi R. Thiol-based copper handling by the copper
624 chaperone Atox1. IUBMB Life 69: 246-254, 2017

625

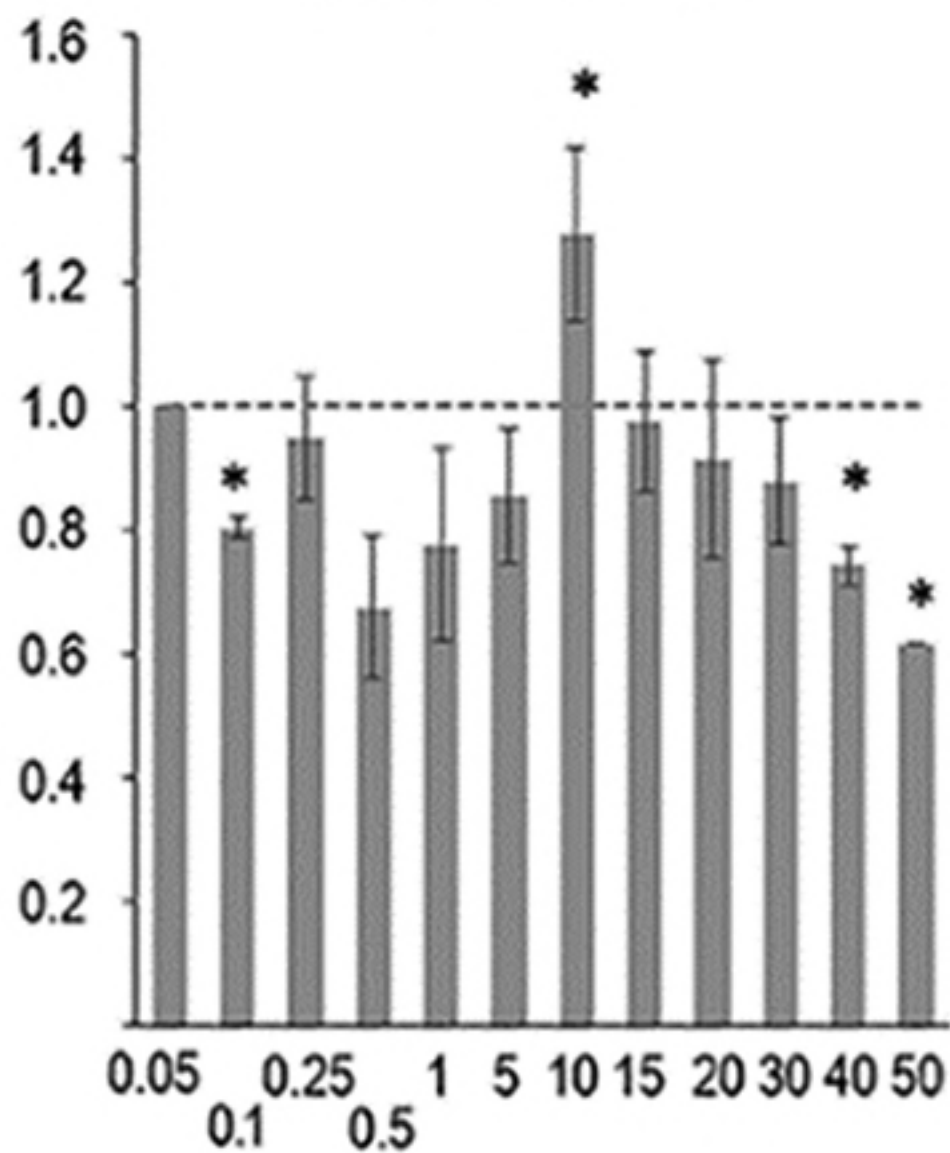
626 **Supplement**

627 **Table S1**

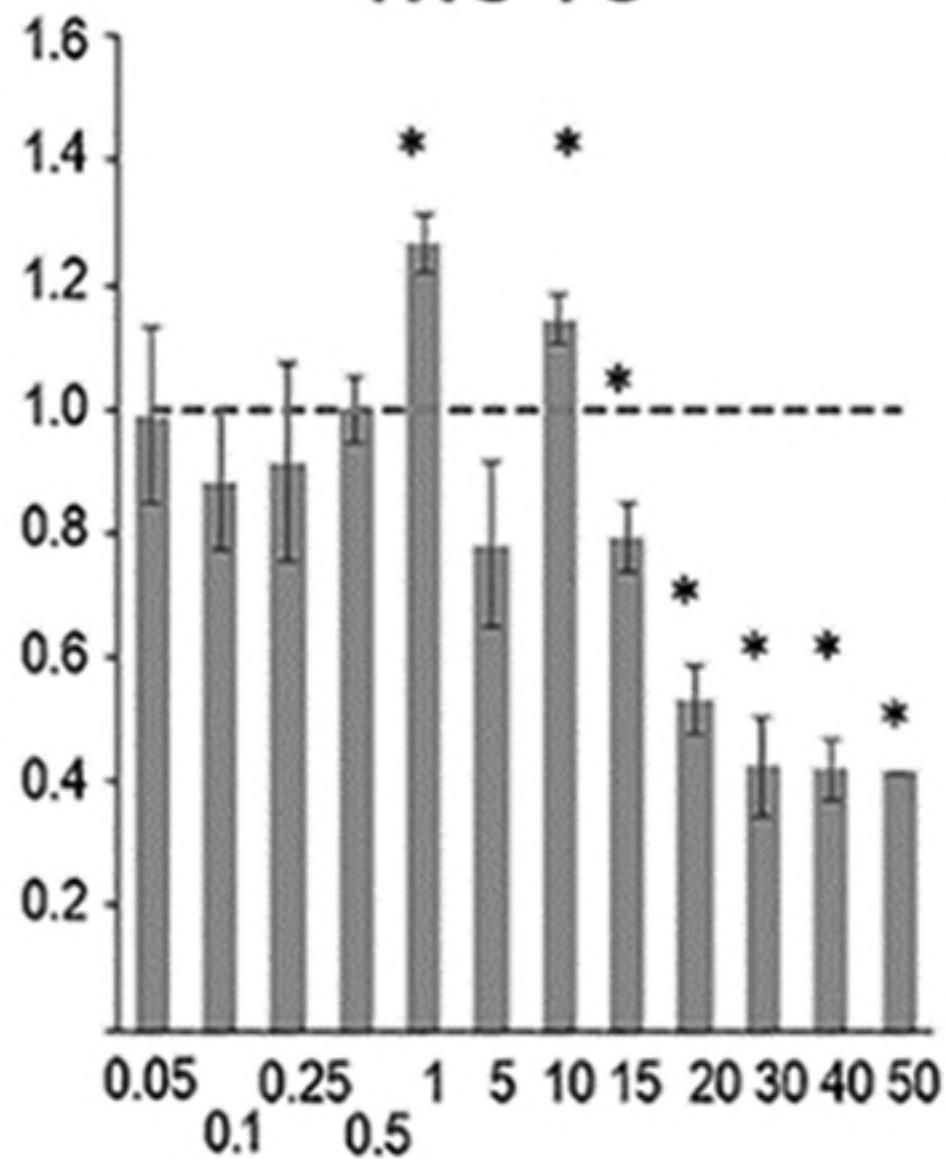
628 **Expression of genes engaged in redox processes in Me45 and HCT116** 629 **cells**

Surviving fraction

HCT116



Me45

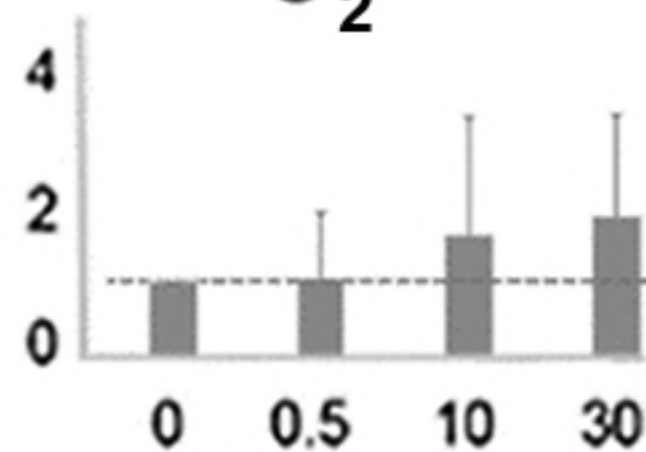


UVA dose [kJ/m²]

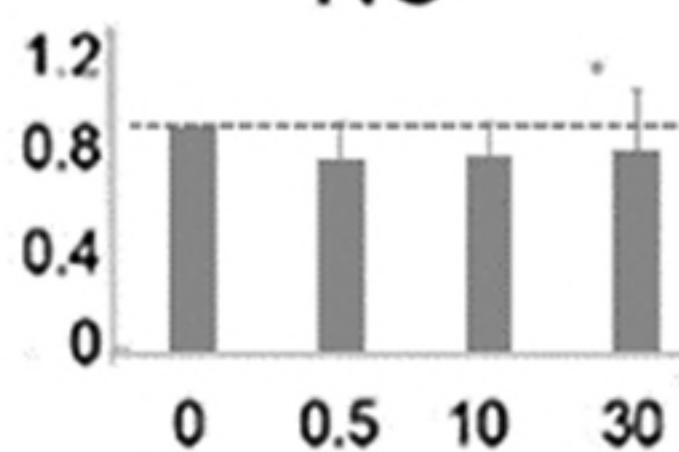
Radical fold change

HCT116

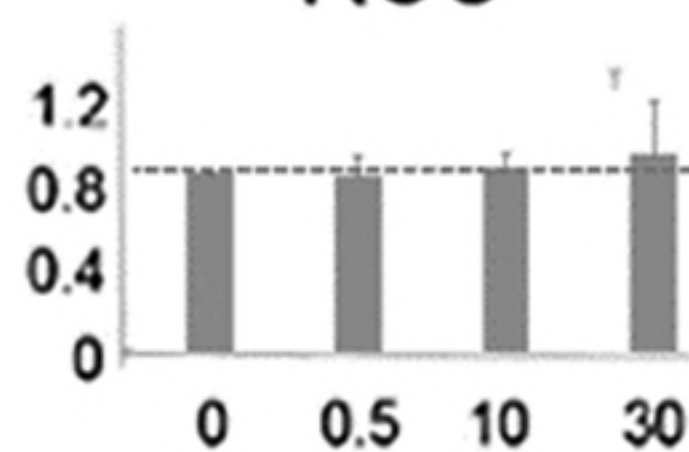
$O_2^{\cdot-}$



NO

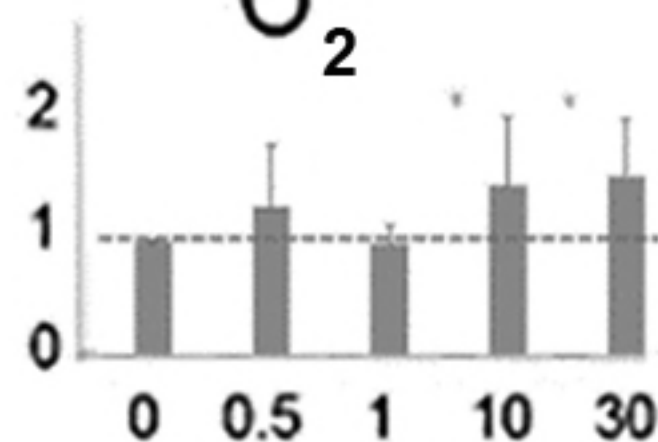


ROS

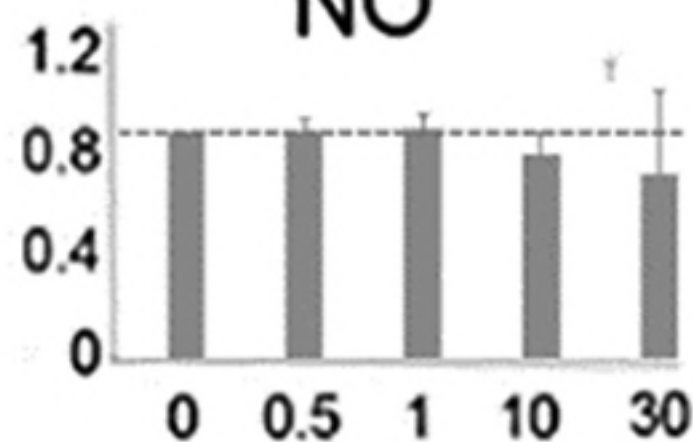


Me45

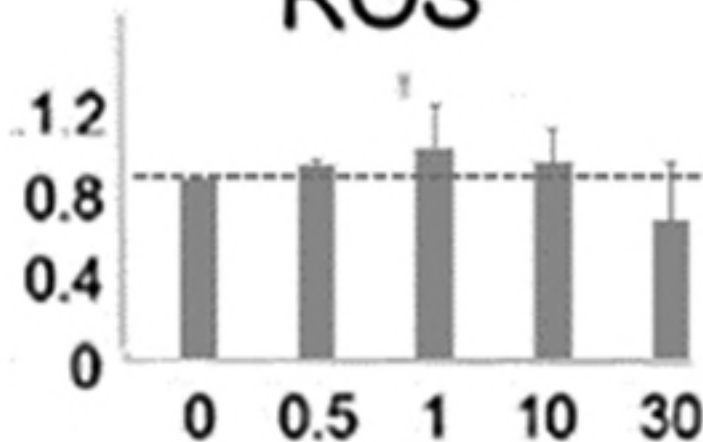
$O_2^{\cdot-}$



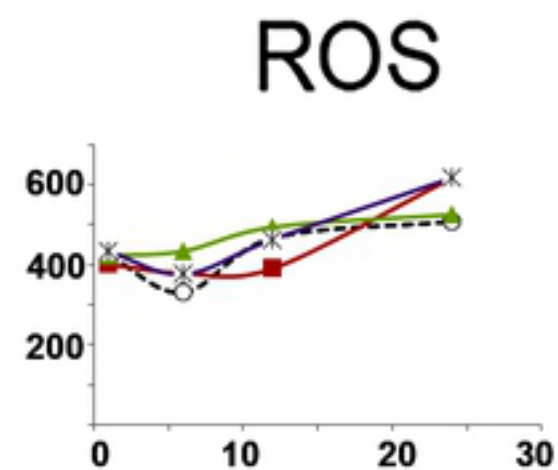
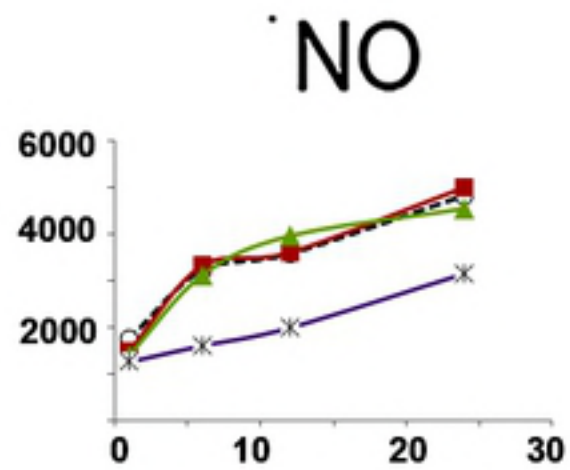
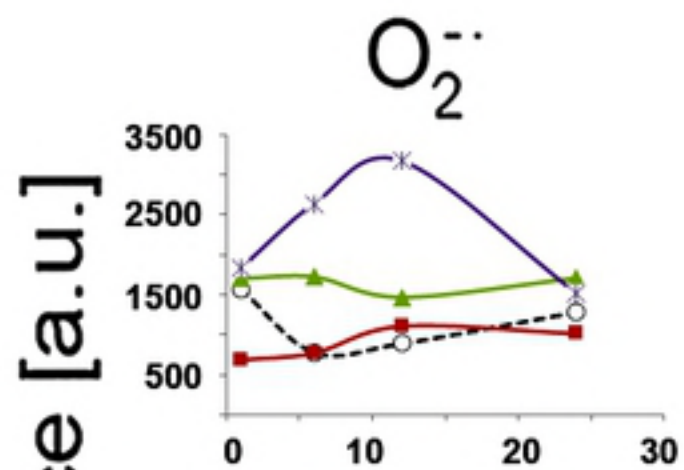
NO



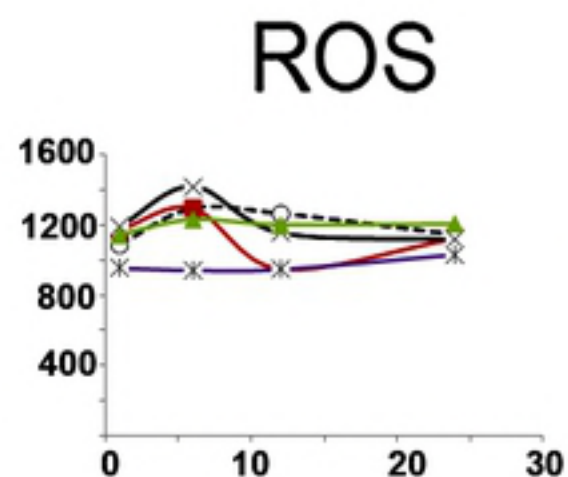
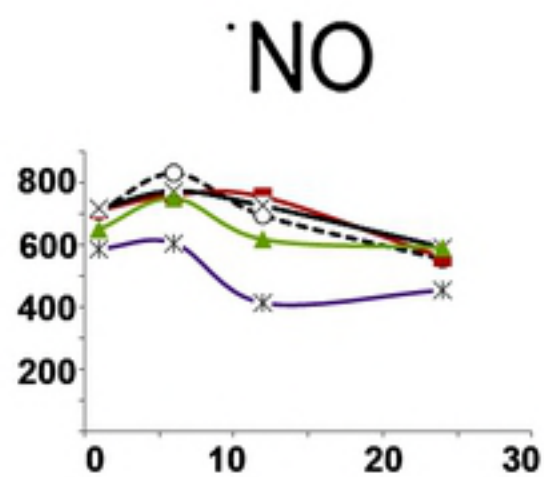
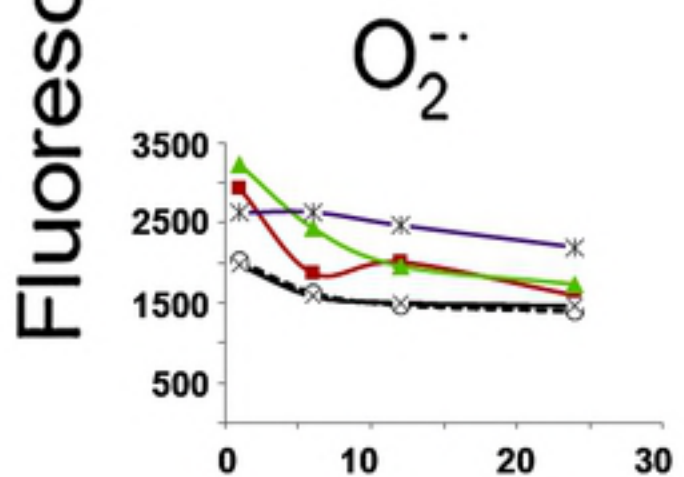
ROS



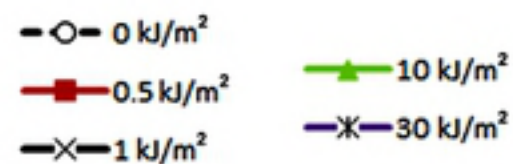
UVA dose [kJ/m²]



HCT116

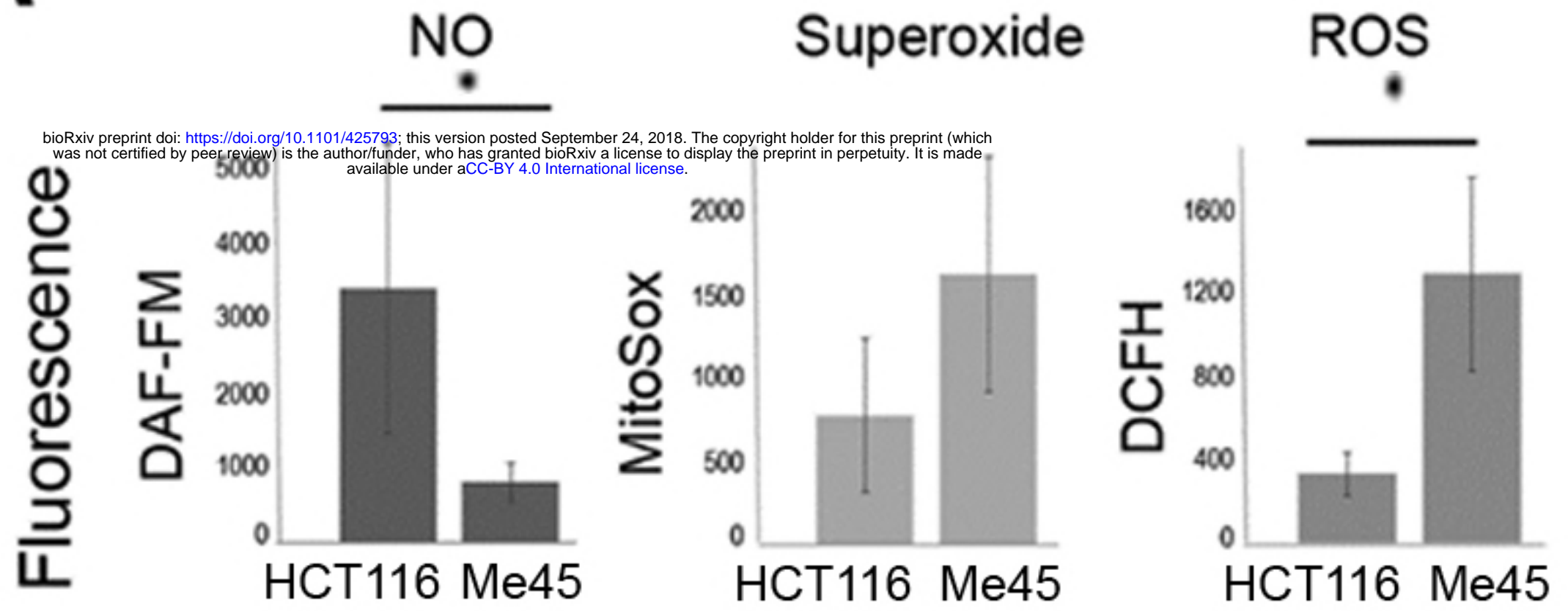


Me45



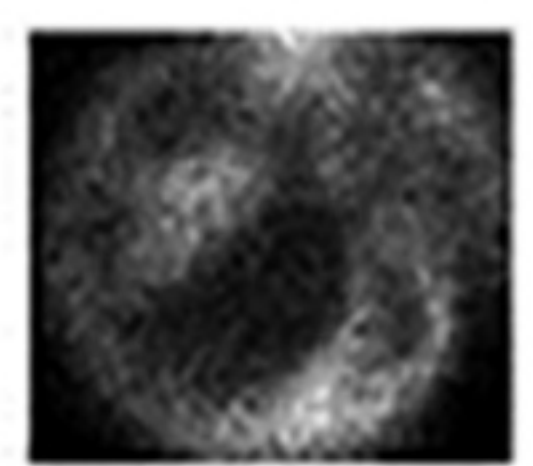
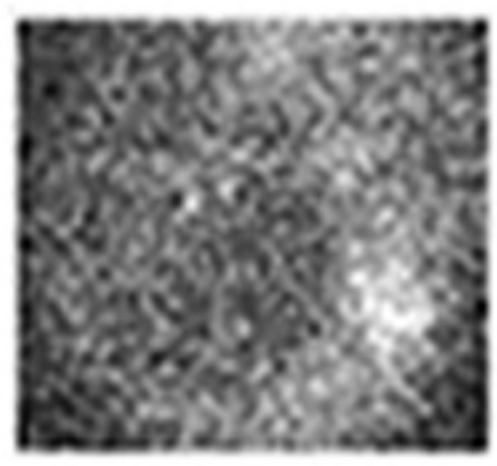
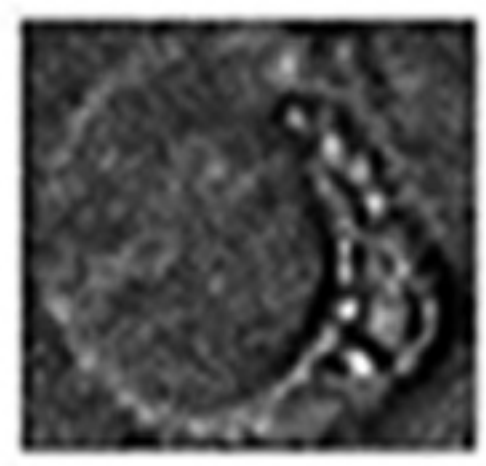
Time [h]

Fluorescence [a.u.]

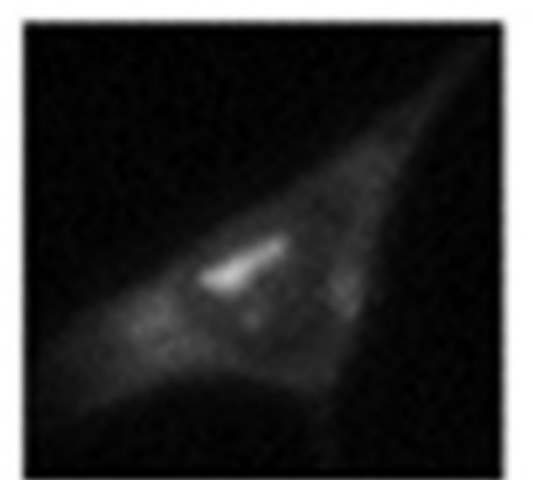
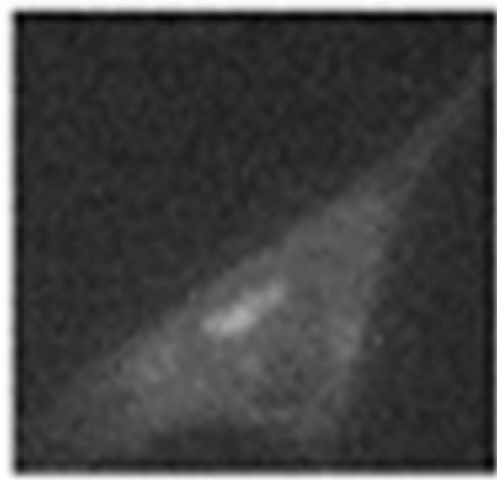
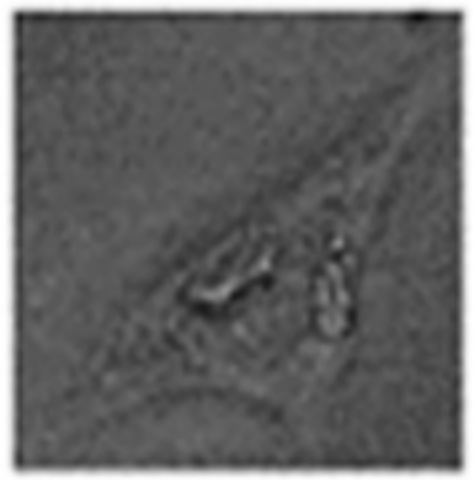
A**B**

Phase contrast NO Superoxide

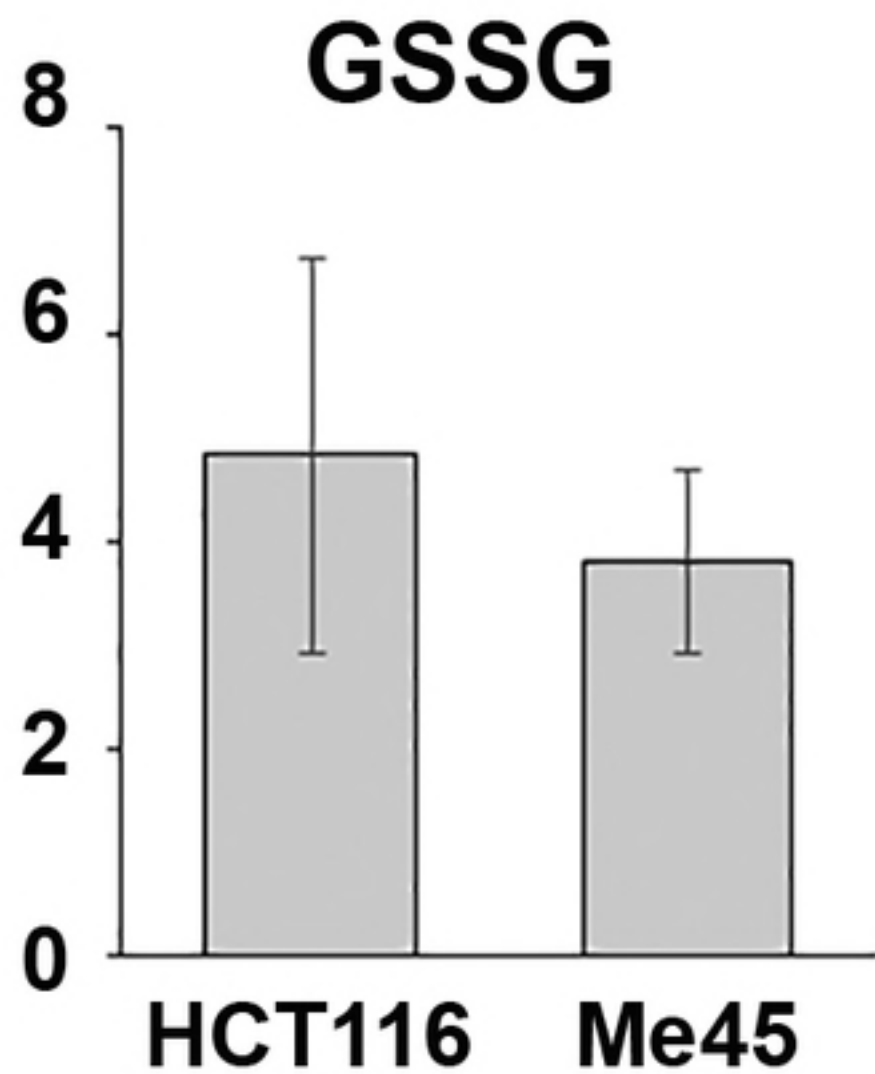
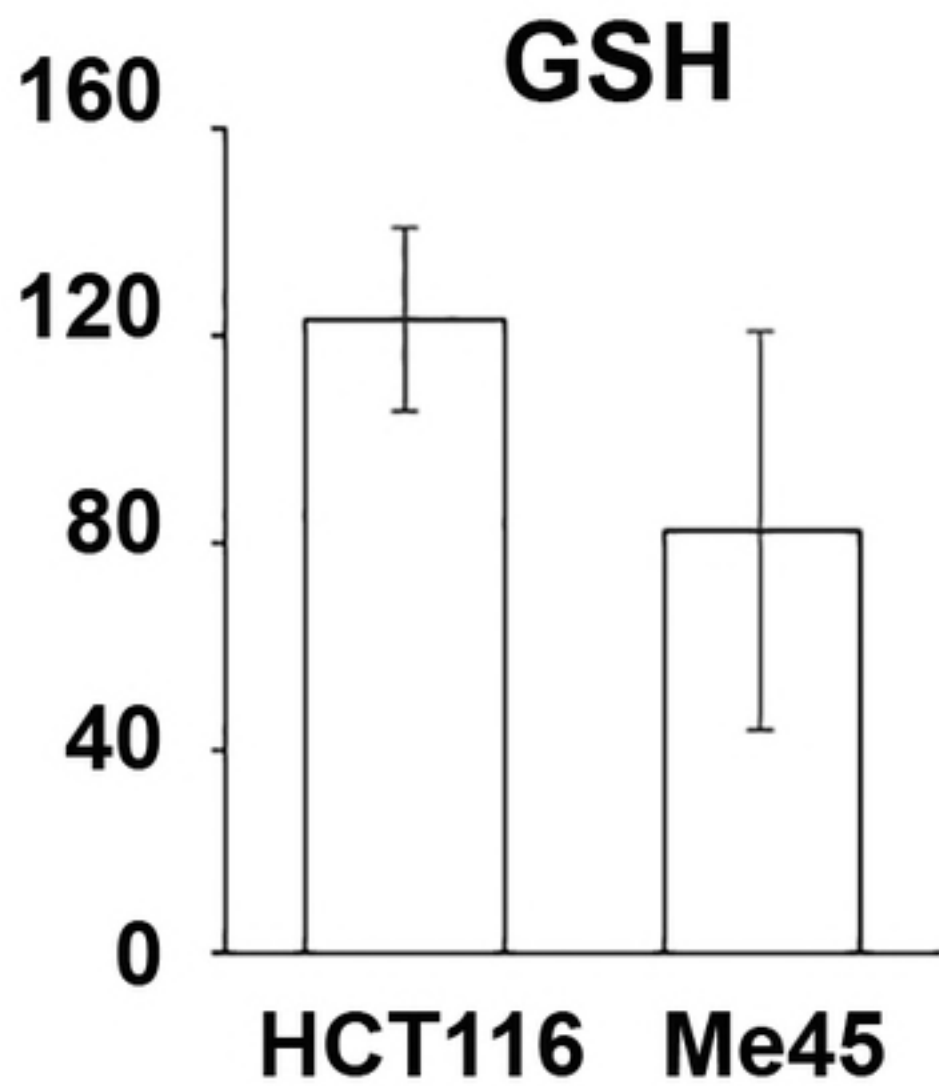
HCT116

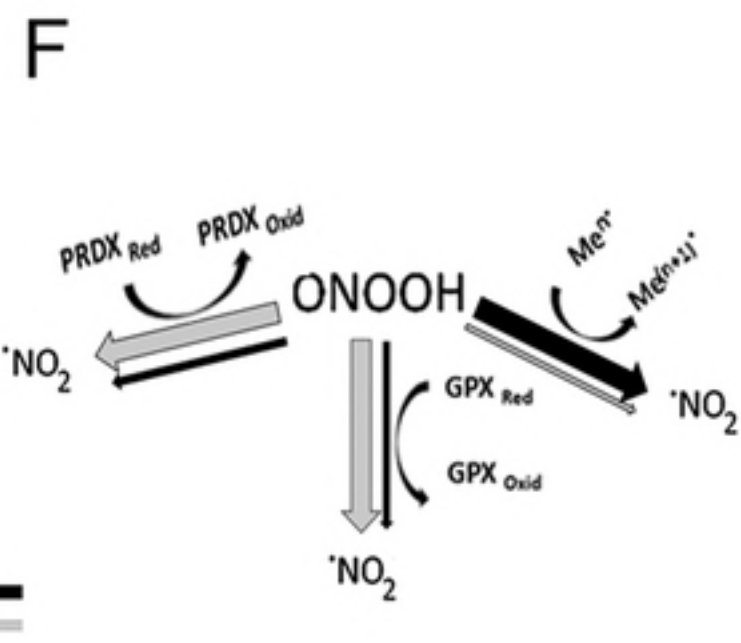
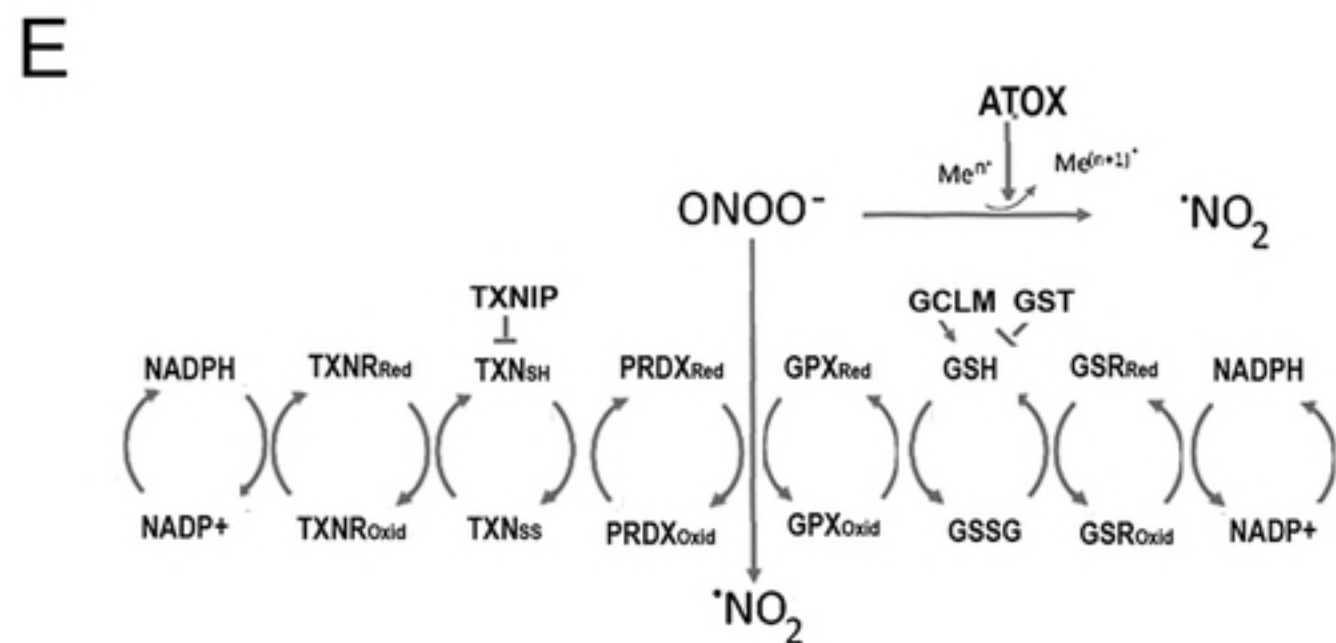
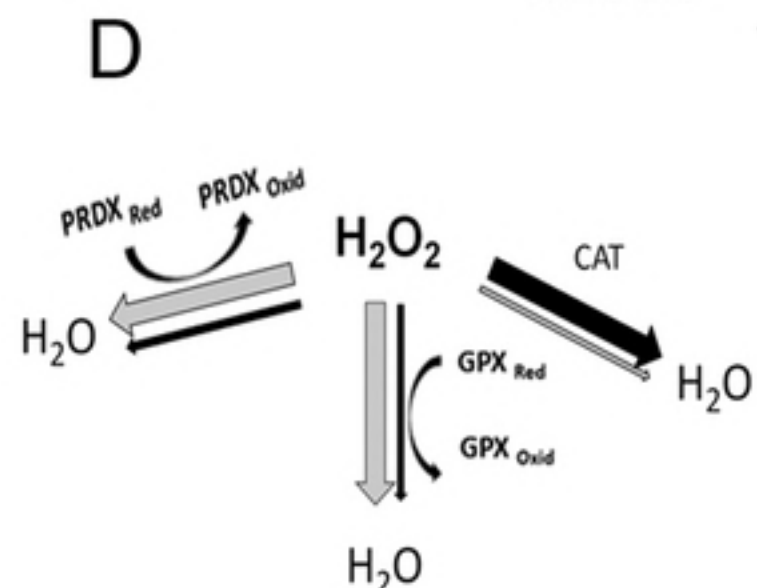
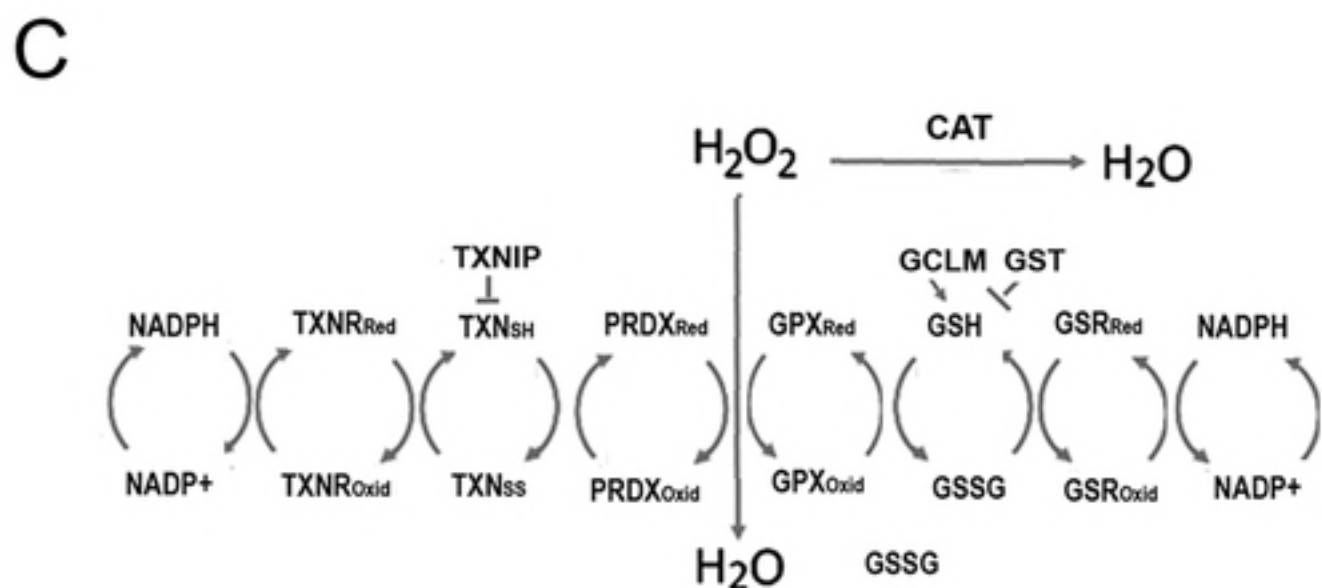
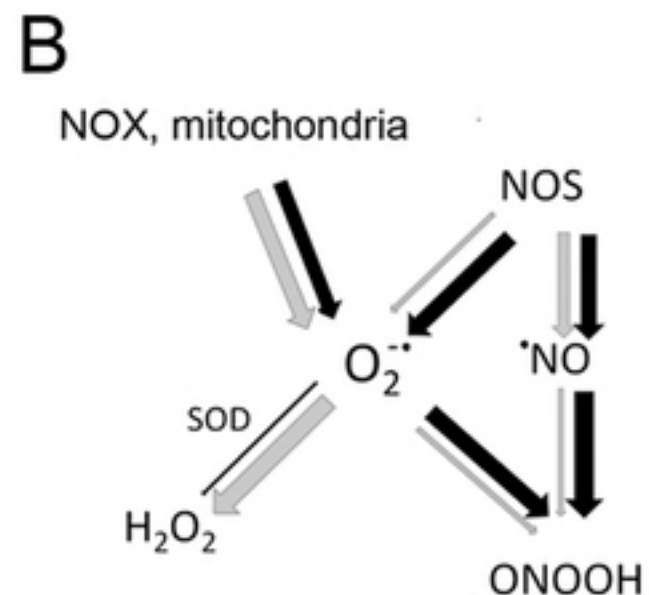
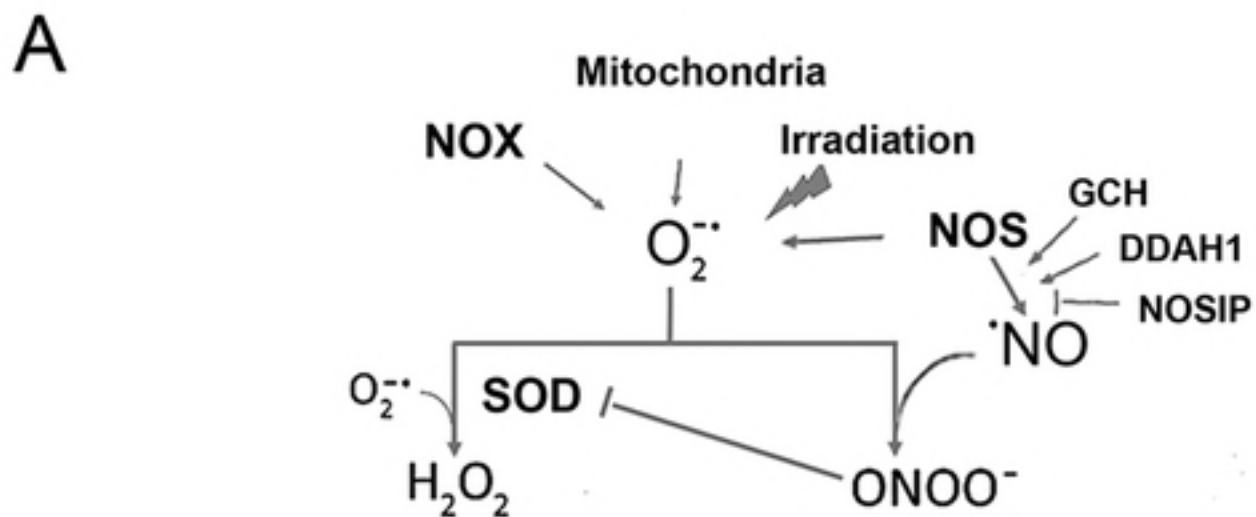


Me45



Glutathione concentration
[nM/mg of protein]





Me45 **—**
HCT116 **—**